

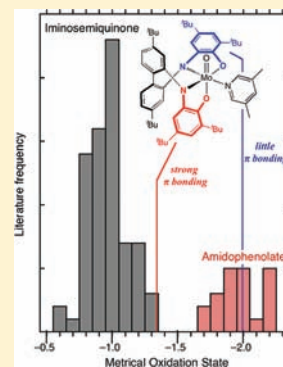
Metrical Oxidation States of 2-Amidophenoxide and Catecholate Ligands: Structural Signatures of Metal–Ligand π Bonding in Potentially Noninnocent Ligands

Seth N. Brown*

Department of Chemistry and Biochemistry, 251 Nieuwland Science Hall, University of Notre Dame, Notre Dame, Indiana 46556-5670, United States

S Supporting Information

ABSTRACT: Catecholates and 2-amidophenoxides are prototypical “noninnocent” ligands which can form metal complexes where the ligands are best described as being in the monoanionic (imino)semiquinone or neutral (imino)quinone oxidation state instead of their closed-shell dianionic form. Through a comprehensive analysis of structural data available for compounds with these ligands in unambiguous oxidation states (109 amidophenolates, 259 catecholates), the well-known structural changes in the ligands with oxidation state can be quantified. Using these correlations, an empirical “metrical oxidation state” (MOS) which gives a continuous measure of the apparent oxidation state of the ligand can be determined based on least-squares fitting of its C–C, C–O, and C–N bond lengths to this single parameter (a simple procedure for doing so is provided via a spreadsheet in the Supporting Information). High-valent d^0 metal complexes, particularly those of vanadium(V) and molybdenum(VI), have ligands with unexpectedly positive, and generally nonintegral, MOS values. The structural effects in these complexes are attributed not to electron transfer, but rather to amidophenoxide- or catecholate-to-metal π bonding, an interpretation supported by the systematic variation of the MOS values as a function of the degree of competition with the other π -donating groups in the structures.

**INTRODUCTION**

Coordination chemists rely heavily on formal oxidation state.¹ In this convention, a central metal ion can be assigned an oxidation state based on charge balance, using the assumption that the ligands bind in a closed-shell form to derive their nominal charges. This assumption generally works well because most ligating atoms are more electronegative than the metals to which they bind, and the resulting metal oxidation states are unambiguous and are often associated with characteristic properties (e.g., Pt(II) is usually square planar). In such cases it makes sense to speak of a “physical” oxidation state of the metal.²

“Noninnocent” ligands, which are readily oxidized or reduced, frustrate this tidy taxonomy and create ambiguities in assigning formal oxidation states.³ Canonical examples of noninnocent ligands are catecholate⁴ and its isoelectronic aza analogues 2-amidophenoxide⁵ and 1,2-diamidobenzene.⁶ An antibonding interaction between the in-phase combination of the heteroatom π lone pairs and one of the benzene π bonding orbitals raises the energy of the highest occupied molecular orbital (HOMO) of the closed-shell, dianionic forms of the ligands,⁷ making them prone to one- or two-electron oxidation to form monoanionic (imino)semiquinones or neutral (imino)benzoquinones (Figure 1). This has led to longstanding interest in the electronic structure of compounds containing these ligands. More recently, the ligands have been explored as electron reservoirs to enable redox chemistry at typically redox-inert metal centers.⁸

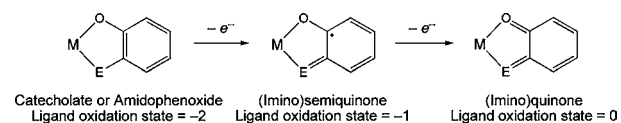


Figure 1. Possible oxidation states of catecholate and amidophenoxide ligands (E = O, NR).

As can be perceived even from the Lewis structures drawn in Figure 1, the oxidation states of these ligands have structural implications. In the dianionic, closed-shell, fully reduced forms, the six-membered ring is aromatic, with C–C bonds intermediate between double and single bonds, and there are carbon-heteroatom single bonds. In the fully oxidized, neutral form, the six-membered ring is quinonoid and there are carbon-heteroatom double bonds. The semiquinone has an intermediate geometry. These geometric changes have been recognized for a long time and have been used extensively in a qualitative fashion to assign the oxidation states of the ligands in metal complexes.^{4,5,9} Similar bond length analyses have been used to assign ligand oxidation states for other redox-active ligands as well.^{10–12}

In a recent study of molybdenum(VI) complexes of a 2,2'-biphenyl-bridged bis(amidophenoxide) ligand, a number of structurally characterized amidophenoxide ligands were ob-

Received: December 26, 2011

Published: January 19, 2012

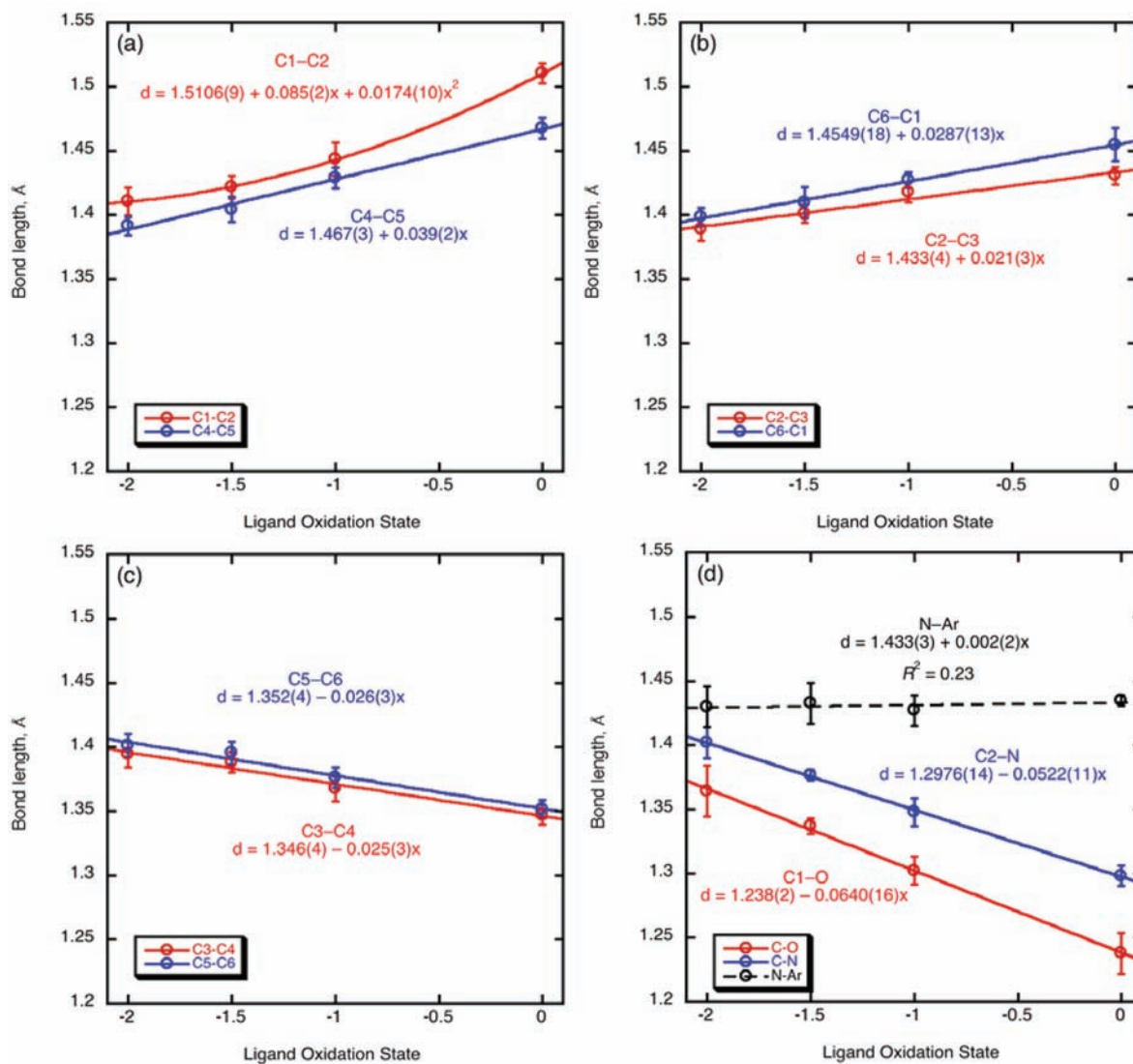


Figure 2. Correlations of bond distances in *N*-arylamidophenoxides with ligand oxidation state: (a) C1–C2 and C4–C5; (b) C2–C3 and C6–C1; (c) C3–C4 and C5–C6; and (d) C1–O, C2–N, and N–Ar (*ipso*). Numbering scheme is as given in Table 1.

served to show perceptible distortions toward a nominal iminosemiquinone oxidation state.¹³ This was difficult to reconcile with all other chemical and spectroscopic features of the molecules, which were entirely consistent with an assignment of oxidation states of Mo(VI) and amidophenoxide(2–). To better illuminate the bonding in these compounds, it was deemed useful to translate the qualitative analyses commonly used into a more quantitative approach, where the metrical data can be interpreted in terms of a single empirical “metrical oxidation state” (MOS) for each ligand. The results of this analysis, and their implications for understanding the bonding in catecholate and amidophenoxide ligands bonded to metals that are strong π acceptors, are described below.

EXPERIMENTAL SECTION

Structural Analysis of Metal Amidophenoxides. From the Cambridge Structural Database (Version 5.31, accessed 5 September 2010) were extracted structures of metal complexes of *N*-aryl-4,6-di-*tert*-butyl-2-amidophenoxide ligands in which the metal oxidation state, and hence the ligand oxidation state, could be inferred with a reasonable degree of certainty. These encompassed compounds of

main group elements (Sn, In, Ga, Sb, Ge), Zn(II), Ni(II), Pd(II), Pt(II), Ir(III), octahedral low-spin Co(III), and octahedral Cr(III). Compounds with an alkyl-substituted or annulated nitrogen substituent (e.g., phenoxazine complexes) were excluded. Complexes of bis(aminophenoxide) ligands with bridges that could potentially be conjugated (e.g., *o*-phenylene) were also excluded, but those with nonconjugated bridges (*m*-phenylene, 2,2'-biphenylene) were included. The data set consisted of 57 structures containing a total of 109 crystallographically distinct ligand fragments (8 with oxidation state 0, 73 with oxidation state –1, 7 with oxidation state –1.5, and 21 with oxidation state –2). References are given in Supporting Information, Table S1, and further details are available in the Supporting Information Microsoft Excel spreadsheet “MOSCalculator.xls”. Nine chemically distinct bond lengths were tabulated for each crystallographically independent ligand molecule in the data set: the C–O and C–N bond lengths, the six C–C bond lengths, and the length of the bond between the nitrogen and the *ipso* carbon of its aryl substituent.

Values were averaged for each oxidation state of the ligand, and the resulting averages were plotted as a function of ligand oxidation state (Figure 2). Linear correlations were adequate to express the observed relationship of distance with oxidation state for the five of the six ring C–C distances, the C–N distance, and the C–O distance. The C1–C2 distance showed a noticeably nonlinear relationship with ligand

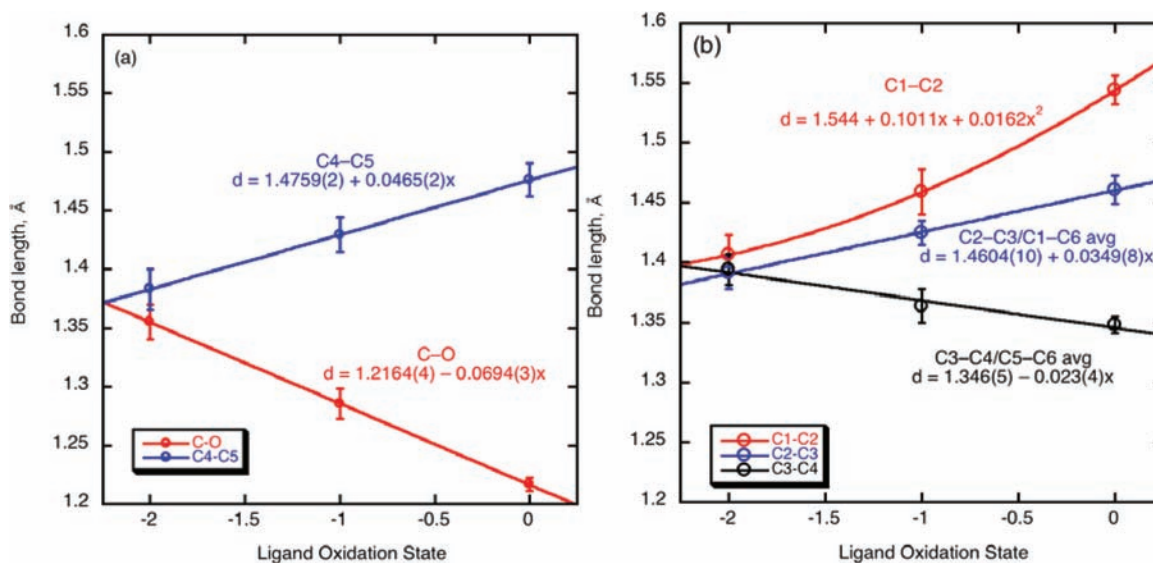
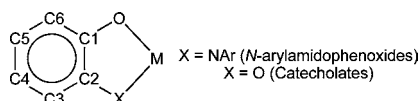


Figure 3. Correlations of bond distances in catecholates with ligand oxidation state: (a) C–O and C4–C5 bonds; (b) C1–C2, C2–C3/C1–C6, and C3–C4/C5–C6 bonds. Numbering scheme is given in Table 1.

Table 1. Average Bond Lengths (Å) for C–C, C–N, and C–O Bonds of Metal *N*-Arylamidophenoxides and Catecholates as a Function of Ligand Oxidation State^a



ligand oxidation state (<i>N</i>) ^b	C–O ^d	C–N	C1–C2	C2–C3 ^d	C6–C1 ^d	C3–C4 ^d	C5–C6 ^d	C4–C5
N-arylamidophenoxides (X = NAr)								
–2 (21)	1.364(20)	1.402(12)	1.411(11)	1.389(9)	1.399(7)	1.395(10)	1.401(9)	1.391(7)
–1.5 (7)	1.337(6)	1.377(4)	1.422(9)	1.401(7)	1.410(12)	1.388(8)	1.395(9)	1.404(10)
–1 (73)	1.302(11)	1.348(11)	1.444(13)	1.418(8)	1.427(6)	1.368(10)	1.376(8)	1.429(8)
0 (8)	1.238(16)	1.298(8)	1.511(8)	1.431(7)	1.455(13)	1.347(8)	1.352(7)	1.468(8)
Catecholates (X = O)								
–2 (146)	1.355(15)	1.406(17)	1.391(13)			1.394(13)		1.383(17)
–1 (74)	1.285(13)	1.459(19)	1.425(10)			1.364(14)		1.429(15)
0 (39) ^c	1.217(6)		1.544(12)	1.461(12)		1.348(7)		1.476(14)

^aStandard deviations of the measured values in the last reported digits are given in parentheses. ^b*N* = number of independent structures with the given oxidation state. ^cDistances at the quinone oxidation state are derived from free organic molecules rather than metal complexes. ^dFor catecholates, the C2–C3 distances and C1–C6 distances are averaged together, as are the C3–C4 and C5–C6 distances and the two C–O distances.

oxidation state but could be described well with a quadratic fit. The quasi-symmetry-related C3–C4 and C5–C6 distances showed identical behavior within the experimental uncertainty; in contrast, the quasi-symmetry-related C1–C6/C2–C3 distances showed similar but not identical behavior. The N–Ar distances showed no significant correlation with ligand oxidation state (slope within one standard deviation of zero, $R^2 = 0.23$), and these values were therefore not analyzed further.

Structural Analysis of Metal Catecholates. Structures from the CSD were again included only if they contained an unambiguous oxidation state for the metal (and hence the catecholate or semiquinone ligands). Only chelating, nonbridging catecholates were included. Compounds with d^0 , d^1 , or d^2 configurations in which π bonding appeared to be possible were excluded. A relatively wide range of substituents were tolerated, but compounds with *ortho* substituents capable of hydrogen bonding (e.g., –CONHR) were excluded, as were benzannulated groups (e.g., phenanthrenequinone derivatives) and compounds with multiple catecholate fragments on a single benzene ring (e.g., dimetalated 1,2,4,5-tetrahydroxybenzene derivatives). As no suitable benzoquinone complexes were identified in the CSD,¹⁴ metrical data for this oxidation state were taken from free

1,2-benzoquinones rather than their metal complexes. A complete list of included structures, with references, is given in Supporting Information, Table S2, and full lists of bond distances are given in the Supporting Information Microsoft Excel spreadsheet “MOSCalculator.xls”.

Tetrachloro- and tetrabromocatecholate ligands were initially considered, but some of their metrical parameters deviated significantly from those of the other catecholates, and they were ultimately excluded. A handful of other electron-poor catecholates, for example, 4-nitrocatecholate, are included in the data set. However, these compounds include some of the most highly discrepant metrical values, so the MOS calculations should therefore not be considered reliable for such electron-poor catecholates.

For each crystallographically unique ligand in the data set, the quasi-equivalent bond lengths (the two C–O lengths; C2–C3 with C1–C6; and C3–C4 with C5–C6) were averaged. Combined with the two unique bond lengths (C1–C2 and C4–C5), this yielded five metrical parameters per ligand. Values were averaged for each oxidation state of the ligand, and the resulting averages were plotted as a function of ligand oxidation state (Figure 3). As for the amidophenoxides, linear

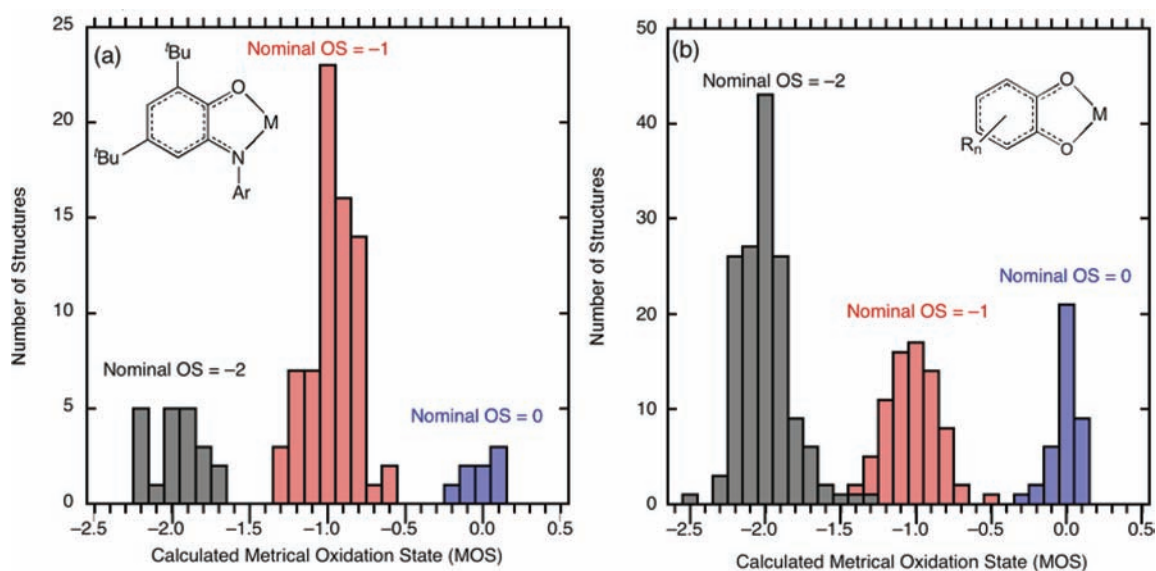


Figure 4. Observed distributions of calculated MOS values for (a) 2-amidophenolate and (b) catecholate complexes.

expressions were used to relate distance to oxidation state except for the C1–C2 distance, which was fit to a quadratic equation.

Calculation of MOS Values. A MOS for each ligand was calculated by unweighted least-squares fitting, minimizing the sum of the squares of the differences between the observed distances in the ligand (eight observables for the amidophenolates, five for the catecholates) and those calculated from the MOS using the equations derived from the analyses of the CSD data. Least-squares minimization was performed using the Levenberg–Marquardt algorithm as implemented in Microsoft Excel¹⁵ with standard deviations of the calculated MOSs calculated by established methods.¹⁶ The calculated MOS values in the calibration set were normally distributed about their nominal oxidation states with mean values and standard deviations of 0.00 ± 0.10 , -0.97 ± 0.15 , -1.56 ± 0.11 , and -1.97 ± 0.17 for the amidophenolates, and 0.00 ± 0.09 , -1.01 ± 0.17 , and -2.01 ± 0.17 for the catecholates. The Supporting Information Microsoft Excel spreadsheet “MOSCalculator.xls” contains simple instructions on how to perform these calculations on any set of amidophenoxide or catecholate bond distances.

Density Functional Theory (DFT) Calculations. Geometry optimizations and orbital calculations were performed on $(\text{PhNC}_6\text{H}_4\text{O})_2\text{ReCl}_2$ and $[(\text{PhNC}_6\text{H}_4\text{O})_2\text{ReCl}_2]^+$ using the hybrid B3LYP method, with an SDD basis set for rhenium and a 6-31G* basis set for all other atoms, using the program Gaussian09.¹⁷ The molecular symmetry of both species was constrained to be C_2 in the calculations. Optimized geometries were confirmed to be minima by frequency analysis. Plots of calculated Kohn–Sham orbitals were generated using the program GaussView (v. 5.0.8) with an isovalue of 0.04.

RESULTS

Metrical Oxidation State (MOS): A Quantitative Interpretation of Structural Trends in Amidophenoxide and Catecholate Ligands. As catecholate or amidophenoxide ligands are oxidized to (imino)semiquinone or (imino)quinone ligands, the carbon-heteroatom and C3–C4 and C5–C6 bonds contract, while the other C–C bonds elongate. These trends are apparent based on a comprehensive analysis of structures reported in the Cambridge Structural Database through 2010 where oxidation states could be unambiguously assigned (Table 1, Figures 2–3). Correlations were satisfactorily described as linear in all cases except that for C1–C2 in the amidophenoxides, where the relationship is clearly nonlinear and was satisfactorily described with a quadratic equation. (The

analogous parameter for the catecholates was also described using a quadratic fit for the sake of parallelism, though the data could also be fit linearly.) While these correlations rely on a more extensive survey of the literature than has previously been undertaken, they are entirely consistent with previous analyses.^{4,5,9} The trends in bond distance clearly reflect the population of the HOMO of the catecholate/amidophenolate. This orbital is strongly antibonding between carbon and the heteroatoms, and strongly bonding between C1 and C2 and between C4 and C5. As the oxidation state increases from -2 to 0 , the population of this orbital decreases from two to zero electrons, and one therefore sees a marked shortening of the carbon-heteroatom bonds and lengthening of the C1–C2 and C4–C5 bonds. Since the contributions of the p orbitals on C3 and C6 to the frontier orbital are small, the effect of oxidation state on the other C–C bond lengths is small as well.

Since each bond length in a catecholate or amidophenoxide complex correlates with the ligand oxidation state, one can predict the bond lengths from the oxidation states. Conversely, given the actual bond distances in a structure, one can calculate an oxidation state for the ligand that would minimize the discrepancies between the predicted and observed distances. The availability of eight observables for amidophenoxides (five for catecholates) should be adequate for determining this single parameter, a metrical oxidation state (MOS) which would represent empirically what oxidation state would best correspond to the observed distances in the given ligand (see the Supporting Information Microsoft Excel spreadsheet for simple implementations of this least-squares fitting procedure). A similar approach, using a much smaller data set, has been applied to 2,6-pyridinediimine ligands to gauge the extent of electron transfer to that ligand.¹⁸

The distances in the compounds used in the training set cluster around their assigned oxidation states, with deviations of the MOS from the initially assigned oxidation state typically less than 0.15 units (Figure 4), and with deviations of greater than 0.3 units being quite rare (4.6%). As an additional test of the reliability of the MOS calculations, the metrical parameters of the relatively abundant neutral homoleptic complexes $\text{Cu}(\text{ArNC}_6\text{H}_2\text{tBu}_2\text{O})_2$ ^{2,19} and $\text{Fe}(\text{ArNC}_6\text{H}_2\text{tBu}_2\text{O})_3$ ²⁰ were computed. These compounds were excluded from the data set used

to generate the correlations because of the potential oxidation state ambiguity of the metals ($\text{Cu}^{\text{II/I}}$, $\text{Fe}^{\text{III/II}}$), but in fact there is general agreement that the oxidation states of the ligands are -1 in both complexes. Mean MOS values calculated for both the Cu complexes (-0.85 ± 0.07 for the 17 crystallographically inequivalent values) and the Fe complexes (-0.86 ± 0.10 for the 24 values) are in satisfactory agreement with this analysis.

Noninteger MOSs in Molybdenum(VI) and Vanadium(V) Complexes. Complexes with metals in high oxidation states ($>+4$) and with two or fewer d electrons were excluded from the data sets. Such compounds may have ambiguous oxidation states and also may experience strong π -donation from the high-lying π orbitals of the catecholate or amidophenoxide ligands. Examples of such complexes are not abundant,²¹ with the most common examples being due to molybdenum(VI) and vanadium(V) complexes. Metrical data from some molybdenum(VI) complexes of amidophenoxides¹³ and catecholates²² (Figure 5) are compiled in Table 2. The

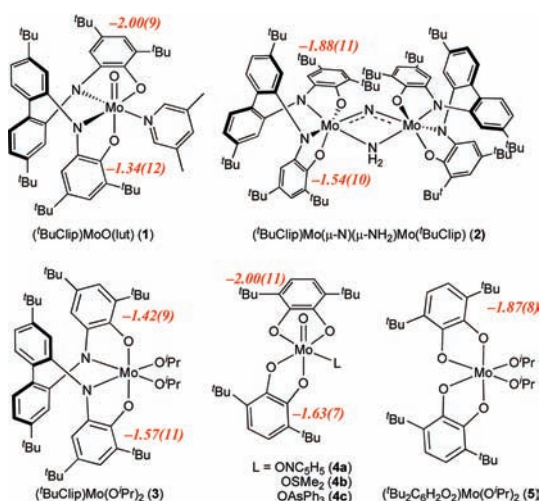


Figure 5. Amidophenolate and catecholate complexes of Mo(VI). Calculated MOS values are shown in italics next to the appropriate rings in the structures.

results of the MOS analysis of the $t\text{BuClip}$ complexes ($t\text{BuClipH}_4 = 2,2'$ -bis(3,5-di-*tert*-butyl-2-hydroxyphenylamino)-4,4'-di-*tert*-butylbiphenyl) indicate that there is modest, but clearly perceptible, variability in their structures. The MOS of the ring trans to the oxo in $(t\text{BuClip})\text{MoO}(\text{lut})$ (1) is $-1.34(12)$, while that of the ring cis to the oxo is $-2.00(9)$. The nitrido complex 2 shows an analogous pattern, but with less variation between the ligands ($-1.57(10)$ and $-1.50(11)$ for the rings trans to the nitride, and $-1.88(12)$ and $-1.87(10)$ for the rings cis to the nitride). The two rings in the isopropoxide complex 3 display MOS values of $-1.42(9)$ and $-1.57(11)$ (while chemically equivalent in solution, the rings experience different environments in the crystal because of the differing conformations of the two alkoxides.¹³) Thus, the amidophenolate groups cis to the multiply bonded ligands show little or no deviation from their expected structures, while the groups trans to the multiply bonded ligands (or trans to alkoxide) do show significant metrical changes consistent with apparent partial oxidation.

Catecholate complexes of molybdenum(VI) show qualitatively similar, though quantitatively more modest, structural effects. Of particular interest are the $(3,6-t\text{Bu}_2\text{C}_6\text{H}_2\text{O}_2)_2\text{MoO}$ -

(L) complexes (L = ONC_5H_5 (4a), OSMe_2 (4b), OAsPh_3 (4c))²² isoelectronic to bis(amidophenolate) complex 1. All three catecholate complexes show structural features very similar to one another, with the cis and trans catecholates differing noticeably (Table 2). As in 1, the cis catecholate shows the expected MOS of $-2.00(11)$; the nonbridging catecholate in $\{\text{Mo}(\text{O})(3,5-t\text{Bu}_2\text{C}_6\text{H}_2\text{O}_2)_2\}_2$, which is cis to the terminal oxo ligand, likewise shows an MOS of $-1.82(15)$, which is not significantly different from -2 .²³ The trans catecholates in 4, in contrast, show noticeable distortions consistent with apparent oxidation (average MOS = $-1.63(7)$), though the effect is smaller than seen in the corresponding amidophenoxide. Similarly, the MOS of the catecholates in the bis(alkoxide) 5²² (MOS = $-1.87(8)$) is not significantly different from -2 , and is more positive than those seen in amidophenolate analogue 3.

In vanadium(V) amidophenoxide complexes (Figure 6), noninteger MOS values are also common. In compounds 6–8,^{20d} the vanadium(V) oxidation state implies an oxidation state of -2 for the amidophenolate ligands. There are two chemically distinct ligands in 6 (four crystallographically inequivalent versions of each) with average calculated MOS values of $-1.37(7)$ for the rings with nitrogens trans to OCH_3 and $-1.72(11)$ for the rings with nitrogens cis to OCH_3 . The single amidophenolate ligand in 7 has a MOS of $-1.59(7)$. In 8, the two chemically inequivalent amidophenolate ligands have average MOS values of $-1.41(8)$ and $-1.68(4)$. In $\text{V}(\text{N}[\text{Ph}]\text{C}_6\text{H}_4\text{Bu}_2\text{O})_3$ (9),^{20d} the assigned $+5$ oxidation state for vanadium would require an average ligand oxidation state of -1.66 ; the observed MOS values are all significantly more positive than this, at $-1.17(10)$, $-1.26(7)$, and $-1.33(6)$. Thus, in all cases, these compounds show significantly more positive MOSs than expected from the formal oxidation state assignment and are not in general close to integer values, very similar to what is observed in the molybdenum amidophenolates.

Vanadium(V) catecholates also typically have a tendency to show noninteger MOS values significantly more positive than -2 (Figure 7), though (as for molybdenum) the effects are more modest than with the amidophenolates. Thus, for example, vanadium(V) tris(catecholate) monoanions have catecholate MOS values of $-1.76(11)$.²⁴ Vanadium(IV) tris(catecholate) dianions do not show appreciable metrical changes, with an average MOS = $-1.96(14)$.²⁵ Neutral and cationic vanadium(V) catecholates typically show larger deviations from -2 (with $(3,5-t\text{Bu}_2\text{C}_6\text{H}_2\text{O}_2)\text{V}(\text{N}_3\text{S}_2)(\text{phen})$ (10) an exception, MOS = $-1.97(8)$ ²⁶). For example, the catecholates in $[(3,5-t\text{Bu}_2\text{C}_6\text{H}_2\text{O}_2)_2\text{V}(\text{phen})]\text{SbF}_6$ (11) have MOS values of $-1.44(12)$ and $-1.39(12)$.²⁷ The neutral complex $(3,6-t\text{Bu}_2\text{C}_6\text{H}_2\text{O}_2)_3\text{V}$ (12), unlike its phenylimino analogue 9, shows a charge-localized structure in the solid state (and apparently in solution),²⁸ with one dioxolene ligand clearly much more distorted than the others and assignable as a semiquinone (MOS = $-1.05(7)$). (The greater tendency of catecholates/semiquinones to charge-localize compared to amidophenolates/iminosemiquinones appears to be a general trend.²⁹) The remaining two ligands, while not as distorted as the semiquinonate, are also perceptibly different from typical catecholates (MOS = $-1.61(4)$). Finally, a number of vanadium(V) oxo-catecholate complexes with tridentate, uninegative ancillary ligands (13) have been structurally characterized.³⁰ These complexes, analogous to the molybdenum complexes 1 and 4, adopt structures with the catecholates

Table 2. MOS Analysis of Molybdenum Amidophenolates and Catecholates^a

ring	C–O	C–N	C1–C2	C2–C3 ^b	C6–C1 ^b	C3–C4 ^b	C5–C6 ^b	C4–C5
(^t BuClip)MoO(lut) ^c								
trans to oxo (Ring 1)	1.316(3)	1.378(4)	1.411(4)	1.418(4)	1.422(4)	1.384(4)	1.375(4)	1.411(4)
<i>calcd</i> , MOS = –1.34	1.324	1.367	1.428	1.405	1.417	1.380	1.387	1.415
Cis to oxo (Ring 4)	1.357(3)	1.415(3)	1.406(4)	1.392(4)	1.403(4)	1.399(4)	1.405(4)	1.390(5)
<i>calcd</i> , MOS = –2.00	1.366	1.402	1.410	1.391	1.397	1.396	1.404	1.389
(^t BuClip)Mo(μ-N)(μ-NH ₂)Mo(^t BuClip) ^c								
trans to μ-N, Ring 1	1.336(3)	1.386(3)	1.398(4)	1.405(4)	1.412(4)	1.377(4)	1.387(4)	1.412(4)
Ring 5	1.332(3)	1.381(3)	1.400(4)	1.399(4)	1.419(4)	1.381(4)	1.384(4)	1.420(4)
<i>calcd</i> , MOS = –1.54	1.338	1.378	1.421	1.401	1.411	1.385	1.392	1.407
Cis to μ-N, Ring 4	1.346(3)	1.415(3)	1.399(4)	1.390(4)	1.402(4)	1.396(4)	1.390(4)	1.400(5)
Ring 8	1.349(3)	1.412(3)	1.402(4)	1.395(4)	1.403(4)	1.393(4)	1.394(4)	1.401(4)
<i>calcd</i> , MOS = –1.88	1.358	1.396	1.412	1.394	1.401	1.393	1.401	1.394
(^t BuClip)Mo(O ⁱ Pr) ₂ ^c								
Ring 1	1.328(3)	1.369(3)	1.404(3)	1.403(3)	1.409(3)	1.377(4)	1.383(4)	1.421(4)
<i>calcd</i> , MOS = –1.42	1.329	1.372	1.425	1.403	1.414	1.382	1.389	1.411
Ring 4	1.337(3)	1.380(3)	1.395(3)	1.402(4)	1.412(3)	1.374(4)	1.385(4)	1.407(4)
<i>calcd</i> , MOS = –1.57	1.339	1.380	1.420	1.400	1.410	1.385	1.393	1.406
(3,6- ^t Bu ₂ C ₆ H ₂ O ₂) ₂ MoO(L) (L = ONC ₃ H ₅ , OSM ₂ , OAsPh ₃) ^d								
trans to oxo	1.332		1.416	1.409		1.382		1.405
<i>calcd</i> , MOS = –1.64	1.330		1.422	1.403		1.383		1.400
cis to oxo	1.363		1.399	1.399		1.391		1.394
<i>calcd</i> , MOS = –2.00	1.355		1.406	1.391		1.391		1.383

^aNumbering system is as given in Table 1. ^bFor catecholates, the C2–C3 distances and C1–C6 distances are averaged together, as are the C3–C4 and C5–C6 distances. ^cData from ref 13. ^dData from ref 22, table entries represent averages of the reported distances from all three structures.

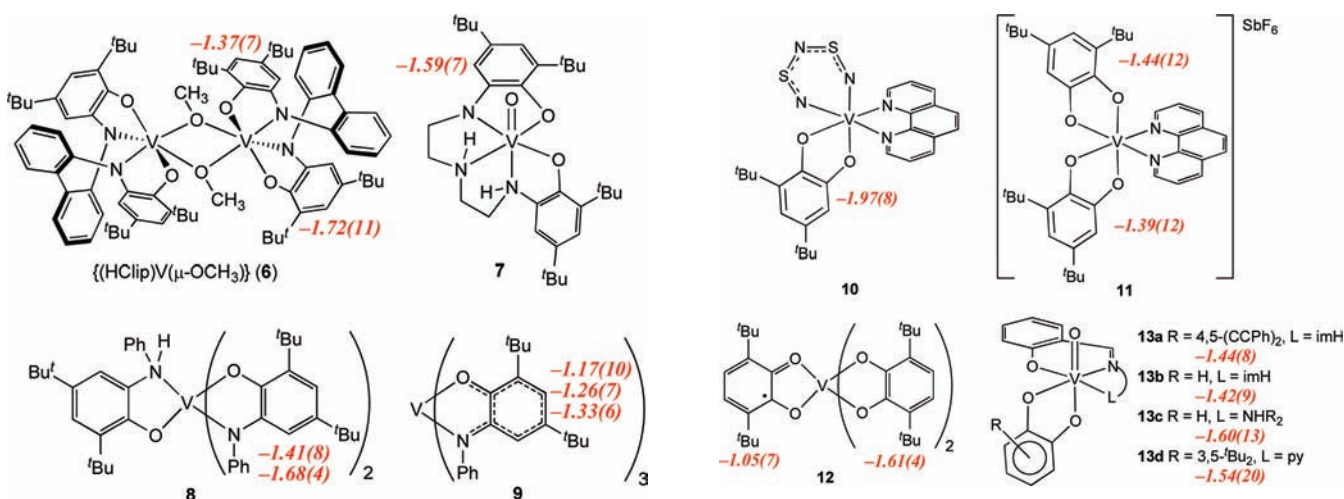


Figure 6. Vanadium(V) amidophenolates. Calculated MOS values are shown in italics next to the appropriate rings in the structures.

trans to the oxo ligand and show catecholate bond distances similar to those shown by the molybdenum trans-catecholates (average MOS = –1.49(9) for the five crystallographically inequivalent structures in four vanadium complexes).

DISCUSSION

Utility of MOS Values for Assessing Bonding in Catecholate and Amidophenoxide Ligands. The bond lengths in catecholates and amidophenoxides have been widely used to assign oxidation states in complexes of these ligands. Typically, the assignments have been based principally on comparison of the carbon-heteroatom bond lengths to benchmark values, with the degree of C–C bond alternation in the ring serving as a secondary indication of ligand oxidation. Because the carbon-heteroatom bonds are quite sensitive to

Figure 7. Vanadium(V) catecholates. Calculated MOS values are shown in italics next to the appropriate rings in the structures.

oxidation state (Figures 2d and 3a), in many cases this approach is satisfactory.

Calculation of MOSs, which is easily done using a least-squares fitting procedure implemented in the Supporting Information Microsoft Excel spreadsheet, improves on this semiquantitative assessment in several ways. The MOS is determined by all eight independent observables (five for catecholates) for each ring and is thus less sensitive to possible errors in any one value. More importantly, by providing a single numerical value for the apparent oxidation state (with an accompanying estimate of error), the MOS calculation allows one to discern variations in structure that are too subtle to detect by qualitative inspection. One must exercise some caution in using the MOS values to determine very small structural variations, since estimated standard deviations in the

values are typically about 0.10 units. As can be seen in the observed distributions of MOS values in Figure 4, even in ligands with unambiguous oxidation states, variations of 0.15 units from the expected values are common and variations of 0.30 units are occasionally observed. But as shown by the analysis of high-valent molybdenum and vanadium compounds, variations that are revealed by MOS calculations to be highly significant, often of 0.4 or more units, have passed without remark in the literature in the absence of such a direct quantitative measure. MOS calculations thus provide a new, general, and useful window into the structure of amidophenoxide and catecholate complexes.

Effects of Metal–Ligand π Bonding on Ligand Structure. The molybdenum and vanadium complexes discussed above were all originally formulated as having the metal in its highest oxidation state. Indeed, assignment of these compounds as Mo(V) or V(IV) makes little chemical sense. Molybdenum(VI) and vanadium(V) with strong π donor ligands are not especially oxidizing. All of the complexes described above are diamagnetic, with the exception of the odd-electron vanadium tris(ligand) complexes, where one ligand must be oxidized even at vanadium(V). Furthermore, the preponderance of *noninteger* values of the MOS is not suggestive of complete electron transfer. Values in the range of -1.3 to -1.7 are typical of the Mo(VI) and V(V) compounds, while unambiguous amidophenolates or catecholates, or (imino)semiquinonates, identified in the CSD almost never show MOS values more than 0.3 away from integer values.

These noninteger values are exactly what is expected if the bond length variations result from amidophenolate- or catecholate-to-metal π donation. The general correlation of bond lengths with oxidation state arises from the fact that the HOMO of the catecholate (or amidophenolate) dianion is antibonding with respect to the carbon-heteroatom and C3–C4/C5–C6 bonds and bonding with respect to the other carbon–carbon bonds in the ring. Depleting the electron density in the HOMO will therefore contract the former bonds and elongate the latter. Any method of depleting the electron density, whether due to electron transfer or π donation to the metal, will have an indistinguishable effect. Since the changes induced by covalency in π bonding are continuous, with more strongly donating ligands (or more strongly π -accepting metal centers) producing greater depletion of electron density, the changes in bonding would likewise vary along a continuum, and noninteger oxidation states should be the norm.

Attribution of the metrical changes to π donation also clearly rationalizes the differences observed between electronically dissimilar ligands in the same complex. For example, in (^tBuClip)MoO(lut) (**1**) or the isoelectronic catecholate complexes **4**, the ring *cis* to the oxo must donate into a $d\pi$ orbital that is already π^* to the oxo ligand, resulting in a poor energy match and little donation. In contrast, the ligand *trans* to the oxo can donate into an otherwise nonbonding d orbital that has δ symmetry with respect to the oxo group (d_{xy} if the $M=O$ vector is along the z axis), resulting in effective donation and a highly delocalized Mo-amidophenolate¹³ or -catecholate π bonding orbital. Similarly, in [(3,5-^tBu₂C₆H₂O₂)₂V(phen)]SbF₆ (**11**), where low-lying $d\pi$ orbitals are available to interact with the catecholate HOMO, MOS values significantly more positive than -2 are observed; in (3,5-^tBu₂C₆H₂O₂)V(N₃S₂)(phen) (**10**), where the N₃S₂³⁻ ligand competes effectively for π bonding to vanadium, the MOS value of the catecholate is

indistinguishable from -2 . In compounds where π bonding is expected to be minimal, such as [Mo^V(O)(3,6-O₂C₆H₂^tBu₂)₂]⁻ (MOS = $-2.01(10)$),²² or is required to be absent by virtue of the 18-electron rule, such as MoH₂(dpep)₂(O₂C₆H₄) (MOS = $-1.95(8)$),³¹ little structural distortion is observed. Finally, a π -bonding explanation for the observed bond lengths makes sense of the variations in structure as the metal or ligand are changed. For example, the more positive MOS values observed for amidophenolates compared to catecholates in analogous compounds are in line with the expectation that the more basic amidophenolate ligand will be a stronger π -donor than the catecholate ligand.

It is important to note that where these compounds have been studied theoretically,¹³ the geometrical features of the ligands are well reproduced by single-determinant, closed-shell singlet DFT calculations. This indicates that while a multi-configurational electronic structure might be invoked as a possible source of noninteger MOSs in some compounds, it is not necessary to do so in the present cases. Indeed, in mid-to-late first-row transition metal complexes of pyridinediimine ligands, whose electronic structures are expected to be much more complicated than those of the Mo and V compounds discussed here, configuration interaction does contribute to geometrical distortions, but even in these first-row compounds, (back)-donation in the closed-shell singlet configuration generally has a greater impact on the observed geometry.¹⁸

Bond distances in catecholate and amidophenoxide ligands have typically been interpreted solely in terms of redox noninnocence, and in many cases this is clearly the sensible interpretation. One could imagine interpreting the bonding in the Mo and V compounds discussed above in this way as well, assigning them as Mo(V) or V(IV) (imino)semiquinonates and invoking strong antiferromagnetic coupling between the odd electron on the metal and that on the ligand. At some level, this is equivalent to a π bonding description; after all, bonding does result in spin pairing of electrons nominally held in separate orbitals with substantial spatial overlap. However, recognizing the effects of bonding explicitly in terms of π interactions, rather than tacitly through antiferromagnetic coupling, is a more useful explanatory model for the present compounds. In particular, a coupled diradical model does not naturally explain the presence of apparent noninteger oxidation states, since spin-pairing does not intrinsically suggest the spatial redistribution of electrons. Bonding, in contrast, requires such spatial redistribution, and polar covalent bonding carries with it the notion that such redistribution will be partial, leading to the *expectation* of noninteger MOSs. Noninteger MOSs can therefore be taken as an indicator of the importance of π bonding. The high-valent Mo and V compounds, where the low d -electron counts and high oxidation state enhance the covalency of the metal–ligand bond and allow strong coupling between metal and ligand orbitals, are well-suited to this qualitative approach and to single-determinant theoretical methods such as DFT. The situation is to be contrasted with more weakly coupled systems typical of later first-row transition elements, where more sophisticated theoretical models may be required to describe the subtler metal–ligand and ligand–ligand interactions.³²

While noninteger MOS values are a strong signal of the likely applicability of a π -bonding model, they are not required by this model, as coincidentally near-integer values may be observed in highly covalent systems. This is illustrated by several high-valent rhenium complexes of 2-(phenylamido)-4,6-di-*tert*-

butylphenoxide (ap) that were described recently (Figure 8).³³ Two (ap)₂Re(O)(X) complexes (X = OC₆Cl₅ (**14a**), Cl (**14b**))

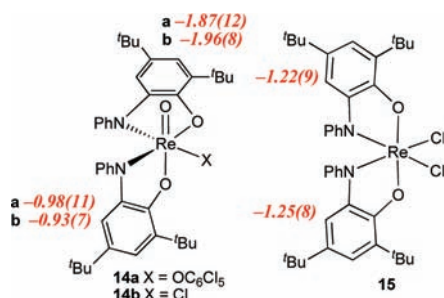


Figure 8. Rhenium amidophenoxide complexes (MOS values in italics).

were prepared and were assigned, based on ligand bond lengths, as containing one dianionic amidophenoxide (cis to the oxo) and one monoanionic iminosemiquinone ligand (trans to the oxo). This interpretation is entirely consistent with quantitative MOS calculations on the compounds (MOS = $-1.87(12)$ and $-1.96(8)$ for the cis ligand and $-0.98(11)$ and $-0.93(7)$ for the trans ligand, for **14a** and **14b**, respectively). These compounds are isoelectronic with (tBuClip)Mo(O)(lut) (**1**, trans MOS = $-1.34(12)$) and are analogous to it both structurally (cis- β geometry, metrically anomalous amidophenolate trans to the oxo) and spectroscopically (diamagnetic with normal ¹H and ¹³C NMR chemical shifts, strong visible absorption). It would therefore seem appropriate that the description of the electronic structure of the rhenium complexes **14** should parallel that of the molybdenum complex **1**. A Re(VII)-bis(amidophenolate) formulation is equally consistent with the metrical data, since Re(VII) would be expected to engage in stronger, more covalent π interactions with the amidophenolate than Mo(VI). One thus need not invoke a radical ligand to explain the metrical data (or spectroscopic observables) in **14**.

In the dichloride complex (ap)₂ReCl₂ (**15**), the ligand bond distances are intermediate between those expected for an amidophenoxide and for an iminosemiquinone, and so the complex was assigned as a mixed-oxidation state amidophenoxide/iminosemiquinonate complex of Re(V), with the odd electron ($\mu_{\text{eff}} = 1.77 \mu_{\text{B}}$) in a ligand-centered orbital.³³ Here, the observed MOS values do differ appreciably from the predicted average values of -1.5 ($-1.22(9)$ and $-1.25(8)$ for the two rings), suggesting that π bonding might be important in this compound. A simple analysis of the bonding in **15** suggests that the two ligand π orbitals interact with two of the metal $d\pi$ orbitals to give two low-lying metal–ligand π bonding orbitals and two high-lying metal–ligand π^* orbitals, with a final metal-centered nonbonding orbital, derived from the third $d\pi$ orbital, in the middle of the energy diagram. This bonding arrangement has been documented theoretically for (acac)₂TiCl₂ (isoelectronic with [(ap)₂ReCl₂]⁺ or the molybdenum bis(alkoxide) complexes **3** and **5**), and the nature of the lowest unoccupied molecular orbital (LUMO) in the titanium complex has been invoked to explain stereoselectivity in binding of ancillary π donors.³⁴ This model predicts that (ap)₂ReCl₂ would have both π bonding levels filled, with one electron occupying the metal-centered nonbonding orbital; the bond distances in the ligands would be ascribed to the substantial π donation to rhenium. This model is supported qualitatively by DFT calculations (see

Supporting Information for details) on both diamagnetic cationic [(PhNC₆H₄O)₂ReCl₂]⁺ (with a LUMO/LUMO+1 gap of 0.28 eV) and paramagnetic neutral (PhNC₆H₄O)₂ReCl₂ (with a predominantly metal-centered singly occupied molecular orbital (SOMO), Supporting Information, Figure S1), though the participation of orbitals other than the five discussed above complicates the detailed description of the bonding. Even here, the character of the SOMO does not distinguish between the bonding models, since an iminosemiquinone/Re(V) formulation with the ligand radical antiferromagnetically coupled with a triplet metal center would also predict a metal-centered SOMO. However, the nature of the coupling pattern is not obvious in such a polyradical model in the absence of detailed calculations. The π -donation model therefore has the advantage that it explains the noninteger MOSs and predicts the character of the SOMO based on simple analyses that give qualitative insights into the bonding in the molecule.

Oxidation states are descriptive conventions rather than physical observables. For transition metals, the usual convention is that, because ligating atoms are typically more electronegative than metals, the ligands adopt closed-shell configurations, with the remaining electrons allocated to the metal center. This convention has been adopted because it is generally useful, and most compounds have unambiguous oxidation states, often with characteristic properties. In such cases one can hope to speak of a “physical” oxidation state of the metal.² No such hope can be held out for the high-valent catecholate and amidophenolate complexes here, as any physical expression of the oxidation state must exist along a continuum because of the covalency of the metal–ligand π interaction. Such compounds can be considered formally as d⁰ complexes of ligand dianions, in line with the usual conventions of coordination chemistry, and if supplemented by an appreciation of ligand-to-metal π donation this provides a satisfactory qualitative description of the bonding in the complexes. An unconventional assignment as d¹ metal/ligand monoanion is not physically distinguishable from this (if likewise supplemented by a description of the bonding between the two electrons) but is less appealing because it is more difficult to perturb this picture in a useful and intuitive way.

In complexes of basic and π -donating ligands such as catecholates and amidophenoxides with high-valent metals with low d electron counts, the availability of high-lying π orbitals on the ligand and low-lying π orbitals on the metal combine to make a delocalized molecule with strong covalent π interactions. The metal and ligand cannot be disentangled from each other and are best thought of as a single conjoined unit. Productive descriptions must bring to the forefront the bonding in the molecules, as this is more important in such strongly coupled systems than whether the electron distributions lie more on the metal or the ligand.

CONCLUSIONS

The well-known correlations between ligand oxidation state C–N, C–O, and C–C bond lengths in amidophenolate and catecholate ligands have been made quantitative based on an analysis of reported structures where these oxidation states can be assigned unambiguously. The distances can be related to a single parameter, a metrical oxidation state (MOS), that represents empirically the oxidation state expected given the bond distances in the ligand and that can be calculated easily using the Supporting Information Microsoft Excel spreadsheet. Compounds of high-valent transition metals such as vanadium-

(V) and molybdenum(VI) often have structures that give MOS values intermediate between the 2- (amidophenoxide/catecholate) and 1- ([imino]semiquinone) oxidation states. These noninteger MOSs are attributed to the partial transfer of electron density from the amidophenoxide/catecholate HOMO to the metal that attends ligand-to-metal π donation. This interpretation is consistent with the trends observed between different ligands within a single complex, where more positive MOS values are seen in ligands that can donate to orbitals that are not already involved in π bonding to strong ancillary π donors such as oxo groups, and between different complexes, where more positive MOS values are found for more strongly donating ligands or more strongly accepting metal centers. The preponderance of noninteger MOS values in such cases flows naturally from the nature of π bonding (which can vary continuously in strength and hence degree of electron depletion in the ligand) and thus serves as a signal that π bonding effects may be important. Clearly, one needs to exercise caution in assigning oxidation states to ligands on the basis of metrical parameters in cases where π interactions are likely to be strong, and such assignments are likely to be less important than the details of the (highly covalent) bonding in the complexes.

■ ASSOCIATED CONTENT

■ Supporting Information

MOS data and calculator (Microsoft Excel spreadsheet), sources for the structural data for the correlations in metal amidophenolates and catecholates and details of DFT calculations (PDF). This material is available free of charge via the Internet at <http://pubs.acs.org>.

■ AUTHOR INFORMATION

Corresponding Author

*E-mail: Seth.N.Brown.114@nd.edu.

■ ACKNOWLEDGMENTS

This work was supported by a grant from the Notre Dame Sustainable Energy Initiative, by the donors of the Petroleum Research Fund, administered by the American Chemical Society, and by the National Science Foundation (CHE-1112356).

■ REFERENCES

- (1) Chirik, P. J. *Inorg. Chem.* **2011**, *50*, 9737–9740.
- (2) Chaudhuri, P.; Verani, C. N.; Bill, E.; Bothe, E.; Weyhermüller, T.; Wieghardt, K. *J. Am. Chem. Soc.* **2001**, *123*, 2213–2223.
- (3) Jørgensen, C. K. *Oxidation Numbers and Oxidation States*; Springer-Verlag: New York, 1968.
- (4) Pierpont, C. G.; Lange, C. W. *Prog. Inorg. Chem.* **1994**, *41*, 331–442.
- (5) Chun, H.; Chaudhuri, P.; Weyhermüller, T.; Wieghardt, K. *Inorg. Chem.* **2002**, *41*, 790–795.
- (6) Lever, A. B. P. *Coord. Chem. Rev.* **2010**, *254*, 1397–1405.
- (7) (a) Gordon, D. J.; Fenske, R. F. *Inorg. Chem.* **1982**, *21*, 2907–2915. (b) Dulatas, L. T.; Brown, S. N.; Ojomo, E.; Noll, B. C.; Cavo, M. J.; Holt, P. B.; Wopperer, M. M. *Inorg. Chem.* **2009**, *48*, 10789–10799.
- (8) (a) Chirik, P. J.; Wieghardt, K. *Science* **2010**, *327*, 794–795. (b) Haneline, M. R.; Heyduk, A. F. *J. Am. Chem. Soc.* **2006**, *128*, 8410–8411. (c) Blackmore, K. J.; Lal, N.; Ziller, J. W.; Heyduk, A. F. *J. Am. Chem. Soc.* **2008**, *130*, 2728–2729. (d) Zarkesh, R. A.; Ziller, J. W.; Heyduk, A. F. *Angew. Chem., Int. Ed.* **2008**, *47*, 4715–4718. (e) Nguyen, A. I.; Blackmore, K. J.; Carter, S. M.; Zarkesh, R. A.;

Heyduk, A. F. *J. Am. Chem. Soc.* **2009**, *131*, 3307–3316. (f) Nguyen, A. I.; Zarkesh, R. A.; Lacy, D. C.; Thorson, M. K.; Heyduk, A. F. *Chem. Sci.* **2011**, *2*, 166–169. (g) Heyduk, A. F.; Zarkesh, R. A.; Nguyen, A. I. *Inorg. Chem.* **2011**, *50*, 9849–9863.

(9) Pierpont, C. G.; Buchanan, R. M. *Coord. Chem. Rev.* **1981**, *38*, 45–87.

(10) (a) de Bruin, B.; Bill, E.; Bothe, E.; Weyhermüller, T.; Wieghardt, K. *Inorg. Chem.* **2000**, *39*, 2936–2947. (b) Bowman, A. C.; Milsmann, C.; Atienza, C. C. H.; Lobkovsky, E.; Wieghardt, K.; Chirik, P. J. *J. Am. Chem. Soc.* **2010**, *132*, 1676–1684. (c) Bowman, A. C.; Milsmann, C.; Bill, E.; Lobkovsky, E.; Weyhermüller, T.; Wieghardt, K.; Chirik, P. J. *Inorg. Chem.* **2010**, *49*, 6110–6123.

(11) (a) Schaub, T.; Radius, U. Z. *Anorg. Allg. Chem.* **2006**, *632*, 807–813. (b) Muresan, N.; Chlopek, K.; Weyhermüller, T.; Neese, F.; Wieghardt, K. *Inorg. Chem.* **2007**, *46*, 5327–5337. (c) Stanciu, C.; Jones, M. E.; Fanwick, P. E.; Abu-Omar, M. M. *J. Am. Chem. Soc.* **2007**, *129*, 12400–12401. (d) Hess, C. R.; Weyhermüller, T.; Bill, E.; Wieghardt, K. *Inorg. Chem.* **2010**, *49*, 5686–5700.

(12) (a) Lu, C. C.; Bill, E.; Weyhermüller, T.; Bothe, E.; Wieghardt, K. *J. Am. Chem. Soc.* **2008**, *130*, 3181–3197. (b) Myers, T. W.; Kazem, N.; Stoll, S.; Britt, R. D.; Shanmugam, M.; Berben, L. A. *J. Am. Chem. Soc.* **2011**, *133*, 8662–8672.

(13) Kopec, J. A.; Shekar, S.; Brown, S. N. *Inorg. Chem.* **2012**, *51*, in press. DOI: 10.1021/ic201736h.

(14) A phenanthrenequinone complex has been characterized, but its benzannulation makes it unsuitable for inclusion in the correlation: Pierpont, C. G.; Downs, H. H. *Inorg. Chem.* **1977**, *16*, 2970–2972.

(15) Harris, D. C. *J. Chem. Educ.* **1998**, *75*, 119–121.

(16) de Levie, R. *J. Chem. Educ.* **1999**, *76*, 1594–1598.

(17) Frisch, M. J.; Trucks, G. W.; Schlegel, H. B.; Scuseria, G. E.; Robb, M. A.; Cheeseman, J. R.; Scalmani, G.; Barone, V.; Mennucci, B.; Petersson, G. A.; Nakatsuji, H.; Caricato, M.; Li, X.; Hratchian, H. P.; Izmaylov, A. F.; Bloino, J.; Zheng, G.; Sonnenberg, J. L.; Hada, M.; Ehara, M.; Toyota, K.; Fukuda, R.; Hasegawa, J.; Ishida, M.; Nakajima, T.; Honda, Y.; Kitao, O.; Nakai, H.; Vreven, T.; Montgomery, J. A., Jr.; Peralta, J. E.; Ogliaro, F.; Bearpark, M.; Heyd, J. J.; Brothers, E.; Kudin, K. N.; Staroverov, V. N.; Kobayashi, R.; Normand, J.; Raghavachari, K.; Rendell, A.; Burant, J. C.; Iyengar, S. S.; Tomasi, J.; Cossi, M.; Rega, N.; Millam, J. M.; Klene, M.; Knox, J. E.; Cross, J. B.; Bakken, V.; Adamo, C.; Jaramillo, J.; Gomperts, R.; Stratmann, R. E.; Yazyev, O.; Austin, A. J.; Cammi, R.; Pomelli, C.; Ochterski, J. W.; Martin, R. L.; Morokuma, K.; Zakrzewski, V. G.; Voth, G. A.; Salvador, P.; Dannenberg, J. J.; Dapprich, S.; Daniels, A. D.; Farkas, O.; Foresman, J. B.; Ortiz, J. V.; Cioslowski, J.; Fox, D. J. *Gaussian 09*, Revision A.02; Gaussian Inc.: Wallingford, CT, 2009.

(18) Budzelaar, P. H. M.; de Bruin, B.; Gal, A. W.; Wieghardt, K.; van Lenthe, J. H. *Inorg. Chem.* **2001**, *40*, 4649–4655.

(19) (a) Mukherjee, C.; Pieper, U.; Bothe, E.; Bachler, V.; Bill, E.; Weyhermüller, T.; Chaudhuri, P. *Inorg. Chem.* **2008**, *47*, 8943–8956. (b) Mukherjee, C.; Weyhermüller, T.; Bothe, E.; Chaudhuri, P. *Inorg. Chem.* **2008**, *47*, 11620–11632. (c) Ye, S.; Sarkar, B.; Lissner, F.; Schleid, T.; van Slageren, J.; Fiedler, J.; Kaim, W. *Angew. Chem., Int. Ed.* **2005**, *44*, 2103–2106.

(20) (a) Mukherjee, S.; Rentschler, E.; Weyhermüller, T.; Wieghardt, K.; Chaudhuri, P. *Chem. Commun.* **2003**, 1828–1829. (b) Dei, A.; Gatteschi, D.; Sangregorio, C.; Sorace, L.; Vaz, M. G. F. *Inorg. Chem.* **2003**, *42*, 1701–1706. (c) Mukherjee, S.; Weyhermüller, T.; Bill, E.; Wieghardt, K.; Chaudhuri, P. *Inorg. Chem.* **2005**, *44*, 7099–7108. (d) Chun, H.; Verani, C. N.; Chaudhuri, P.; Bothe, E.; Bill, E.; Weyhermüller, T.; Wieghardt, K. *Inorg. Chem.* **2001**, *40*, 4157–4166.

(21) Some group IV *N*-alkylamidophenolate complexes have been structurally characterized. While the quantitative values should be treated with caution, since the correlations were developed with only *N*-aryl complexes, the MOS values for $(\text{BuNC}_6\text{Bu}_2\text{H}_2\text{O})_2\text{M}(\text{THF})_2$ are Ti, MOS = -1.88(7); Zr, MOS = -1.95(9); Hf, MOS = -1.98(7); (a) Blackmore, K. J.; Ziller, J. W.; Heyduk, A. F. *Inorg. Chem.* **2005**, *44*, 5559–5561. (b) Blackmore, K. J.; Sly, M. B.; Haneline, M. R.; Ziller, J. W.; Heyduk, A. F. *Inorg. Chem.* **2008**, *47*, 10522–10532.

- (22) Liu, C.-M.; Nordlander, E.; Schmeh, D.; Shoemaker, R.; Pierpont, C. G. *Inorg. Chem.* **2004**, *43*, 2114–2124.
- (23) Buchanan, R. M.; Pierpont, C. G. *Inorg. Chem.* **1979**, *18*, 1616–1620.
- (24) Yin, C.-X.; Finke, R. G. *J. Am. Chem. Soc.* **2005**, *127*, 9003–9013.
- (25) Milsman, C.; Levina, A.; Harris, H. H.; Foran, G. J.; Turner, P.; Lay, P. A. *Inorg. Chem.* **2006**, *45*, 4743–4754.
- (26) Kabanos, T. A.; Slawin, A. M. Z.; Williams, D. J.; Woollins, J. D. *J. Chem. Soc., Chem. Commun.* **1990**, 193–194.
- (27) Kabanos, T. A.; White, A. J. P.; Williams, D. J.; Woollins, J. D. *J. Chem. Soc., Chem. Commun.* **1992**, 17–18.
- (28) Morris, A. M.; Pierpont, C. G.; Finke, R. G. *Inorg. Chem.* **2009**, *48*, 3496–3498.
- (29) Pierpont, C. G. *Inorg. Chem.* **2011**, *50*, 9766–9772.
- (30) (a) Kraft, B. J.; Coalter, N. L.; Nath, M.; Clark, A. E.; Siedle, A. R.; Huffman, J. C.; Zaleski, J. M. *Inorg. Chem.* **2003**, *42*, 1663–1672. (b) Cornman, C. R.; Kampf, J.; Pecoraro, V. L. *Inorg. Chem.* **1992**, *31*, 1981–1983. (c) Cornman, C. R.; Colpas, G. J.; Hoeschele, J. D.; Kampf, J.; Pecoraro, V. L. *J. Am. Chem. Soc.* **1992**, *114*, 9925–9933. (d) Baruah, B.; Das, S.; Chakravorty, A. *Inorg. Chem.* **2002**, *41*, 4502–4508.
- (31) Minato, M.; Sakai, H.; Weng, Z.-G.; Zhou, D.-Y.; Kurishima, S.; Ito, T.; Yamasaki, M.; Shiro, M.; Tanaka, M.; Osakada, K. *Organometallics* **1996**, *15*, 4863–4871.
- (32) (a) Neese, F. *Coord. Chem. Rev.* **2009**, *253*, 526–563. (b) Boyer, J. L.; Rochford, J.; Tsai, M.-K.; Muckerman, J. T.; Fujita, E. *Coord. Chem. Rev.* **2010**, *254*, 309–330.
- (33) Lippert, C. A.; Hardcastle, K. L.; Soper, J. D. *Inorg. Chem.* **2011**, *50*, 9864–9878.
- (34) (a) Brown, S. N.; Chu, E. T.; Hull, M. W.; Noll, B. C. *J. Am. Chem. Soc.* **2005**, *127*, 16010–16011. (b) Kongprakaiwoot, N.; Quiroz-Guzman, M.; Oliver, A. G.; Brown, S. N. *Chem. Sci.* **2011**, *2*, 331–336.